NASA TECHNICAL NOTE

NASA TN D-8045 e.1

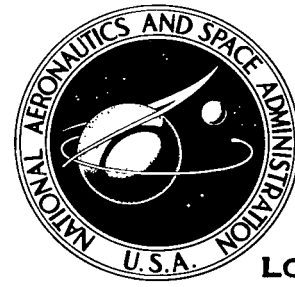

NASA TN D-8045

LIFE ANALYSIS OF HELICAL GEAR SETS USING LUNDBERG-PALMGREN THEORY

John J. Coy and Erwin V. Zaretsky

Lewis Research Center
and U.S. Army Air Mobility R&D Laboratory
Cleveland, Ohio 44135

NATIONAL AERONAUTICS AND SPACE ADMINISTRATION • WASHINGTON, D. C. • AUGUST 1975

1. Report No.	2. Government Accession No.	3. Recipient's Catalog No.
NASA TN D-8045		

4. Title and Subtitle
LIFE ANALYSIS OF HELICAL GEAR SETS USING LUNDBERG-PALMGREN THEORY

5. Report Date
August 1975

6. Performing Organization Code

7. Author(s)
John J. Coy and Erwin V. Zaretsky

8. Performing Organization Report No.
E-8283

9. Performing Organization Name and Address
NASA Lewis Research Center and
U.S. Army Air Mobility R&D Laboratory
Cleveland, Ohio 44135

10. Work Unit No.
505-04

11. Contract or Grant No.

12. Sponsoring Agency Name and Address
National Aeronautics and Space Administration
Washington, D.C. 20546

13. Type of Report and Period Covered
Technical Note

14. Sponsoring Agency Code

15. Supplementary Notes

16. Abstract

A mathematical model is developed for surface fatigue life of helical gears. The expected fatigue life of a pinion, gear, or gear set may be calculated from the model. An equation for the dynamic capacity of a gear set was also derived. Dynamic capacity is the transmitted tangential load which gives a 90 percent probability of survival of the gear set for one million pinion revolutions. The equations, when simplified by setting the helix angle to zero, reduce to the results which were previously developed for spur gears. A sample calculation is given which illustrates the use of the new fatigue life model.

17. Key Words (Suggested by Author(s))	18. Distribution Statement
Gears; Transmissions; Fatigue life; Reliability; Lubrication; Machine design	Unclassified - unlimited STAR Category 37 (rev.)

19. Security Classif. (of this report)	20. Security Classif. (of this page)	21. No. of Pages	22. Price*
Unclassified	Unclassified	33	$3.75

* For sale by the National Technical Information Service, Springfield, Virginia 22161

CONTENTS

LIFE ANALYSIS OF HELICAL GEAR SETS USING LUNDBERG-PALMGREN THEORY

by John J. Coy and Erwin V. Zaretsky

Lewis Research Center and
U.S. Army Air Mobility R&D Laboratory

SUMMARY

A mathematical model for surface fatigue life of helical gears was developed. The derivation is based on the Lundberg-Palmgren theory, which has been accepted since 1950 as the best predictor of rolling-element bearing life. In addition, an equation for the dynamic capacity of a gear set was derived. Dynamic capacity is defined as the transmitted tangential load which gives a 90 percent probability of survival of the gear set for one million pinion revolutions. It was assumed that the gears were geometrically ideal with no profile errors or tooth spacing errors. The effect of dynamic loads induced by tooth flexibility and gear inertia was neglected. Uniform line contact between mating gear teeth was assumed. The influence of stressed volume and gear tooth flexibility are discussed.

The sample calculation given uses material constants obtained from rolling-element bearing tests and the Weibull slope from gear tests.

INTRODUCTION

Gears used in power transmissions may fail in several different ways - such as tooth breakage caused by high bending stresses in the gear teeth, scoring of the gear tooth surface due to an inadequate lubricant film, or surface pitting caused by high surface-contact stress (ref. 1).

Blok first postulated in 1937 (ref. 2) that there is a critical or flash temperature below which no scoring takes place. This phenomenon is discussed further in reference 3. The prevailing opinion today is that scoring resistance of gear teeth may be improved by making changes in gear lubricant or gear tooth profiles (refs. 1 and 4). If these changes are successful in lowering the temperature in the conjunction zone between

the meshing gears, the scoring resistance will be improved (ref. 3).

Design methods for avoiding gear tooth breakage are based on the bending endurance limit of the gear material. Usually, in these methods the helical gear tooth is analyzed as a cantilevered beam with the addition of semiempirical service and geometry factors. If the maximum calculated bending stress is less than the bending endurance limit of the material, it is presumed that no tooth breakage will occur (refs. 5 and 6). More exact calculations of the stress in bending have been made by finite element methods. The results are compared in reference 7 with American Gear Manufacturers' Association (AGMA) and International Standard Organization (ISO) standards on the strength of gear teeth. However, this reference deals only with spur gear teeth. In 1960, Wellauer and Seireg presented a semiempirical method for analyzing the helical gear tooth as a cantilevered plate. The results were incorporated into a strength rating for helical gears (refs. 8 and 9).

Current methods of design to resist surface fatigue are based on the concept of a surface fatigue endurance limit. The current method (refs. 10 and 11) of predicting gear tooth pitting failures is similar to that used for predicting tooth breakage. According to this method the Hertzian contact stress is estimated and then modified by service condition and geometry factors to become the stress number. By definition, when the stress number is less than the surface fatigue endurance limit, no surface pitting failures will occur.

Gear life tests and roller life tests are reported in reference 12. Based on experiment, the authors state that there appears to be no surface fatigue endurance limit. They are of the theoretical opinion, however, that there is a surface fatigue endurance limit. Schilke (ref. 13) and Huffaker (ref. 14) are convinced that there is no endurance limit for surface fatigue. This has also been the position of the rolling-element bearing industry since the publication of two important papers by Lundberg and Palmgren in 1947 and 1952 (refs. 15 and 16).

Recently, several authors have applied statistical methods to predicting gear life. A probabilistic method of deciding the allowable stress from a small amount of fatigue test data is presented in reference 17. The method depends on the existence of a surface fatigue endurance limit. Bodensieck (ref. 18) presents a stress-life-reliability system for rating gear life. His work is a nontraditional approach intended to give more precision to life and reliability predictions. Work has been done recently wherein the theory of Lundberg and Palmgren was applied to gear surface fatigue (refs. 19 and 20). The experimental life obtained from fatigue testing of vacuum-arc-remelted (VAR) AISI 9310 gears was reported in reference 20. A life theory for surface pitting of spur gears was also derived. The theoretical and experimental lives were in good agreement. Also experimental life studies have been conducted to determine the failure distribution of spur gears under various conditions (refs. 12 to 14, 20, and 21). Unfortunately, there are no similar experimental data for helical gears.

The research reported herein was conducted to extend the spur gear failure theory presented in reference 20 to helical gears. This extension uses the basic pitting fatigue failure theory of Lundberg and Palmgren, which has been proven valid for rolling-element bearings for the past two decades. It is assumed herein that helical gear life is a function of the stressed volume, the critical stress, and the depth of occurrence of the critical stress as determined for the helical gear. This assumption is the same as those for the spur gears (ref. 20) and rolling-element bearings (refs. 15 and 16).

FATIGUE THEORY

The fatigue life model proposed in 1947 by Lundberg (ref. 15) is the commonly accepted theory for determining the fatigue life of rolling-element bearings. In reference 20 the basic theory of Lundberg and Palmgren was applied to obtain the surface fatigue life of a single spur gear tooth. The formulation obtained was based on the assumption of a uniformly distributed load on the line of contact between the meshing spur gear teeth. But the spur gear formulation is not applicable to helical gears because they differ in geometry from spur gears. The helical inclination of the gear teeth causes a gradual shifting of the transmitted load from one tooth to the next as the teeth pass through the plane of action. This fact makes it necessary to review the assumptions regarding maximum stress and stressed volume in deriving a fatigue life model for helical gears. In appendix B it is shown how the following basic model for surface fatigue life is derived from the Lundberg-Palmgren theory:

$$L_1 = \left(\frac{K_1 z_o^h}{\tau_o^c V} \right)^{1/e} \tag{1}$$

where

L_1 life of gear tooth, millions of revolutions

K_1 material constant for a 90 percent probability of survival

z_o depth of occurrence of critical stress

τ_o critical stress

V volume representation of stress concentration or "stressed volume"

e Weibull's exponent

h, c material-dependent exponents

(All symbols are defined in appendix A.) The material constant K_1 used in this report is ultimately based on life data obtained by Lundberg and Palmgren for AISI 52100 steel with hardness of Rockwell C 60. For newton and meter (SI) units, $K_1 = 1.428 \times 10^{95}$; for pound and inch (U.S. customary) units, $K_1 = 3.583 \times 10^{56}$.

In the following sections, helical gear geometry and gear tooth loads are used to determine the critical stress and the stress field. The results may be used with equation (1) to give the gear life equation in terms of familiar gear design parameters.

MAXIMUM HERTZIAN CONTACT STRESS

At this time there is no exact stress analysis in the literature for a helical gear tooth. Finite element methods have been applied to spur gear teeth (ref. 7), but there is no similar work for helical gear teeth.

Current helical gear design practice is to estimate the stress at the pitch point of the teeth by assuming line contact between two cylinders whose radii depend on the curvature of the helical gear teeth at the pitch point. The unit loading on the contact line is estimated by assuming that the teeth are infinitely rigid and that the load is distributed uniformly along the line of contact (refs. 22 and 23).

Another method of calculating load distributions, by Matsunaga (ref. 24), is based on the assumption of a constant deflection of the teeth in mesh at any point on the line of contact. His calculations use an extension of the semiempirical "moment image" method of Wellauer and Seireg (ref. 8). Matsunaga's calculations show a $2\frac{1}{2}$:1 variation in the theoretical unit loading across the contact line. However, the method of calculation neglects Hertzian and beam shearing deformations. He also notes from his gear tests that when pitting occurred it was near the pitch line of the driving member. It is interesting that the highly loaded regions (according to ref. 24) were near the lowest point of contact on the pinion. Matsunaga's opinion is that scoring wear relieved the high stress in that area. Hence, the region near the pitch point became more highly stressed, causing the resulting pitch-line pitting to occur.

For purposes of calculating contact stress, it is assumed that the pitch point is the most highly loaded area. There are two reasons for this assumption. First, a fatigue spall requires both a high contact stress and a certain number of stress cycles for its formation. There is evidence that pitch-line pitting is not dependent on prior scoring wear that alters the involute tooth form (ref. 21). Second, tooth load sharing in spur gears causes the heaviest loads to occur near the pitch point. The same effect probably occurs for helical gears, mainly because of the higher bending compliance of the gear tooth as the load nears the tooth tip.

Figure 1 shows the necessary geometry for estimating the Hertzian contact stress

at the pitch point. Based on these assumptions the maximum Hertzian contact stress is calculated by the formula (ref. 20)

$$q = \frac{2}{\pi b}\left(\frac{Q}{\ell_c}\right) \tag{2}$$

where ℓ_c is the length of the contact line. For spur gears this length is the same as the face width in contact. However, for helical gears, as shown in figure 2, this is not the case. For this reason the work done for spur gears in reference 20 is not directly applicable to helical gears. The equation for the semiwidth of the contact (ref. 20) is

$$b = \sqrt{\frac{8Q}{\pi \ell_c E_o \sum \rho}} \tag{3}$$

CONTACT LINE LENGTH

The zone of contact in the plane of action is shown in figure 2. Several lines of contact for mating pairs of teeth lie in the zone of contact. The process that takes place can be imagined as a series of slanting lines (the contact lines) passing through a stationary viewing frame (the plane of action). The total length of the lines of contact ℓ_c may be calculated at each instant of time by graphical or analytical methods. Figure 3 shows the typical variation in the length of the contact lines that occurs during the gear meshing process. For gears with good helical action, ℓ_c is equal to approximately 95 percent of the average total length of the contact lines (ref. 10).

$$\ell_c = 0.95 \frac{\zeta f}{p_b \cos \psi_b} \tag{4}$$

The Hertzian stress varies inversely with the square root of ℓ_c. While it is recognized that the Hertzian stress is not constant over the entire cycle of contact, it is felt that no large errors in approximation will be introduced since it can be shown that gear life is inversely proportional to load to approximately the 1.5 power. Therefore, a 10-percent increase in load results in a decrease in life of approximately 13 percent.

For helical gears of low axial contact ratio, equation (4) becomes less accurate. Its use should be reserved for gears with axial contact ratios near 2. If the axial contact ratio is much less than 2, ℓ_c should be calculated from the geometry of figure 2.

STRESSED VOLUME

The expression for the stressed volume is derived in appendix C as

$$V = \frac{3}{4} f z_o \ell \sec \psi_b \tag{5}$$

where z_o represents the depth under the surface at which the critical stress acts and ℓ denotes the length of involute in the critically loaded zone.

At this time it is not clear whether the maximum orthogonal reversing shear stress or the maximum shear stress should be considered as the critical stress (ref. 25). The value of the maximum shear stress and its depth below the surface are affected by relative sliding between the contacting bodies (ref. 26). This sliding affects the traction coefficient. The authors of reference 27 are of the opinion that the fatigue life of ball bearings is reduced by increases in traction. Their data show a reduction in life by a factor of 3 when the traction coefficient increases from 0 to 0.0675. According to the results presented in reference 19, there is no noticeable reduction in life with increased traction for the roller disk test machine. However, much more data must be collected before a definite conclusion may be drawn.

One interesting observation can be made from the stress analysis of Smith and Liu (ref. 26). For traction coefficients larger than 1/9, the maximum shear stress lies on the surface. If the z_o associated with this stress is used in equation (5), the stressed volume vanishes. This would result in no life at all according to equation (1). It is significant also that the peak-to-peak amplitude of the reversing orthogonal shear stress does not change its magnitude or position below the surface for increased traction coefficients. In view of the aforementioned, it is probably best at this time to adhere strictly to the original intent of Lundberg and Palmgren and use the orthogonal reversing shear stress as the critical or decisive stress. However, the critical stress actually may be the maximum shear stress or the orthogonal shear stress. These stresses may be affected by the increased amount of sliding in the helical gear mesh (ref. 26). If at some future time this proves to be the case, the theory may be readily modified by a "percent of sliding" term.

For spur gears the length ℓ was taken as the length of involute for which a single pair of teeth were in contact. For helical gears there is no equivalent length because of the gradually changing nature of the load sharing between the teeth. Therefore, several choices of length are possible depending on which assumption seems most reasonable for a particular situation. The simplest method of choosing ℓ would be to use the entire length of involute for which there is tooth action. This would be consistent with the assumption that the helical teeth are infinitely rigid and that the only variation in tooth

loading is caused by the changing length of the contact line, as described in the previous section. A second possible method is to choose the length ℓ equal to ℓ_1, where the ℓ_1 is calculated as for a spur gear by using transverse plane geometry. This calculation is outlined in reference 20.

The second method is consistent with the assumption that the helical teeth can be modeled as spur teeth which are slightly displaced from one another along the helix angle, as shown in figure 4. It is further assumed that the adjacent spur sections cause no increase in stiffness of the elemental spur section. Therefore, to a degree, these two methods are extremes which bracket the true load-sharing ability of the helical gear teeth. The results should provide reasonable lower and upper bounds to the statistical analysis of the life of a helical gear set.

LIFE AND DYNAMIC CAPACITY

As a first step in determining gear mesh life, an equation which gives the life of a single tooth for 90 percent reliability was developed in a form that depends on the gear parameters that are familiar to most mechanical engineers. By using equations (1) to (3), (5), (B7), and (B8) the following results were obtained:

$$L_1 = \left[\frac{K_1 \left(\frac{2}{\pi}\right)^{(h-1)/2} (32\pi)^{c/2} \left(\frac{4}{3}\right) \left(\frac{Q}{\ell_c}\right)^{(h-c-1)/2} \cos \psi_b}{f\ell \left(E_o \sum \rho\right)^{(h+c-1)/2}} \right]^{1/e} \tag{6}$$

The terms in equation (6) can be simplified or written in terms of more familiar parameters of the helical gear geometry. From figure 1 the load Q, which lies in the plane of action and is normal to the contact line, may be written in terms of the transmitted tangential load which acts normally to the line of centers at the pitch point.

$$Q = \frac{W_t}{\cos \psi_b \cos \varphi_t} \tag{7}$$

The curvature sum at the pitch point may be written as

$$\sum \rho = \frac{\cos \psi_b}{\sin \varphi_t} \left(\frac{r_1 + r_2}{r_1 r_2} \right) \tag{8}$$

By using equations (7) and (B13) to (B15) in equation (6), the following expression is obtained:

$$W_t L_1^{2e/(c-h+1)} = K_2 \ell_c \cos \varphi_t \left[f\ell (\cos \psi_b)^{(h-c-3)/2} \left(\sum \rho \right)^{(h+c-1)/2} \right]^{2/(h-c-1)} \tag{9}$$

where $K_2 = 132\ 000$ when pound and inch units are used and $K_2 = 5.28 \times 10^8$ when newton and meter units are used, for a material similar to AISI 52100 steel of Rockwell C 60 hardness. By definition the dynamic capacity of a single pinion tooth is the transmitted tangential load W_{tP} that may be carried for one million pinion revolutions with a 90 percent probability of survival. From equation (9)

$$W_{tP} = K_2 \ell_c \cos \varphi_t \left[f\ell (\cos \psi_b)^{(h-c-3)/2} \left(\sum \rho \right)^{(h+c-1)/2} \right]^{2/(h-c-1)} \tag{10}$$

The life of the single pinion tooth for a given transmitted load is

$$L_1 = \left(\frac{W_{tP}}{W_t} \right)^p \tag{11}$$

where

$$p = \frac{c - h + 1}{2e} \tag{12}$$

The next step in the derivation is to develop the lives and dynamic capacities for the entire pinion, the gear tooth, and the entire gear and finally for the system which is composed of the gear and pinion in mesh. This derivation was performed in reference 20. The results are presented in equations (13) to (20). The lives listed will be expressed in terms of millions of pinion revolutions. For the pinion,

$$L_P = N_1^{-1/e} L_1 \tag{13}$$

For a single gear tooth in terms of pinion rotations,

$$L_{2P} = \left(\frac{N_2}{N_1} \right)^{(1+e)/e} L_1 \tag{14}$$

For the gear,

$$L_{GP} = N_2^{-1/e} L_{2P} = N_2 N_1^{-(1+e)/e} L_1 \tag{15}$$

For the mesh of gear and pinion,

$$L_M = \left\{ N_1 \left[1 + \left(\frac{N_1}{N_2} \right)^e \right] \right\}^{-1/e} L_1 \tag{16}$$

The dynamic capacity of the gear tooth is given by

$$W_{tG} = \left(\frac{N_2}{N_1} \right)^{(1+e)/w} W_{tP} \tag{17}$$

where

$$w = \frac{c - h + 1}{2} = pe \tag{18}$$

For the gears in mesh the dynamic capacity is

$$W_{tM} = \left\{ N_1 \left[1 + \left(\frac{N_1}{N_2} \right)^e \right] \right\}^{-1/w} W_{tP} \tag{19}$$

If the actual transmitted tangential load is W_t, the corresponding life is given by

$$L = \left(\frac{W_{tM}}{W_t} \right)^p \tag{20}$$

Most of the terms in these equations are on any standard dimension sheet for the helical gear. However, as was previously pointed out, ℓ_c and ℓ, which are the length of the contact line and the length of the involute in the critically loaded region, respec-

tively, are not as readily determined. The approximate minimum contact-line length ℓ_c may be found directly from equation (4), or the true minimum contact-line length may be found from a tedious analysis of figure 2. Also, as mentioned previously, there are several choices for the length of involute ℓ to be used in equation (10). Appendix D gives some gear geometry that is useful in computing ℓ.

NUMERICAL EXAMPLE AND DISCUSSION

The theory is now used in a sample calculation for the life and dynamic capacity of a helical gear drive. Assume that the drive consists of a 16-tooth pinion and a 36-tooth gear. The input speed is 1000 rpm and 3000 kW (4000 hp) are transmitted. The gears have a 0.0762-meter (3-in.) face width. The diametral pitch is 0.3937 tooth/cm (1 tooth/in.). The tooth form has the basic proportions given by table 5-16 (tooth form 1) in reference 28. It is assumed that the gear material is case-hardened steel of Rockwell C 60 hardness. The values $h = 2\frac{1}{3}$ and $c = 10\frac{1}{3}$, taken from rolling bearing test data, are used. The Weibull slope $e = 3$ was determined from NASA tests of AISI 9310 steel spur gears (ref 20).

Expected life was calculated for each of two different assumptions regarding the failure-causing stress pattern on the gear tooth surface. In case I, it was assumed that the peak Hertzian stress acts over the region of the tooth for which there is single-tooth contact if the helical gear is imagined as shown in figure 4. The following expression is true for case I:

$$\ell_c = \frac{f}{\cos \psi_b} \tag{21}$$

In case II, the contact-line length ℓ_c was calculated by equation (4), and it was assumed that the peak Hertzian stress acts over the entire region for which the teeth are in contact. In this sample calculation the face width is small compared to the axial pitch. As the ratio of the face width to axial pitch becomes smaller, the amount of helical tooth overlap also decreases. This is the case for gears used in automotive transmissions. Marine reduction gears are much wider, having a greater amount of helical action. Therefore, while both cases I and II give reasonable lower and upper bounds to the life prediction, case I is probably the more accurate assumption.

The details of the calculation are presented in table I, and the predicted failure distribution is plotted on Weibull coordinates in figure 5. Weibull coordinates are the log-log of the reciprocal of the probability of survival graduated as the statistical percentage of specimens failed (ordinate) against the log of the time to failure or system life (ab-

scissa). The calculated upper and lower bounds of the 10-percent life (90 percent probability of survival) are 890 and 1050 hours. The maximum contact stress for case I is 119 000 N/cm^2 (173 000 psi). When the conditions of this problem are used to calculate gear life according to AGMA gear surface durability standards (ref. 10), an infinite life is predicted. The bending-induced stress calculated according to reference 5 is only 16 000 N/cm^2 (23 000 psi), giving a safety factor of about 2 for the bending fatigue type of failure.

There is a design guide (ref. 29) used for the purpose of improving the accuracy of life predictions for rolling-element bearings. The guide accounts for life improvement due to quality of lubrication and material improvements in the steels used. It is possible to apply some of these life adjustment factors to gear-life prediction. Further, as data from helical gear fatigue tests become available, the material constant and exponents may be determined with greater accuracy. It may also become possible to determine the influence of dynamic loading and sliding, which has been neglected in the present analysis.

SUMMARY OF RESULTS

Equations for the dynamic capacity and life of helical gear sets were developed. The failure mode was assumed to be surface fatigue pitting. The dynamic capacity is the transmitted tangential load which will give a 90 percent probability of survival of the gear set for one million pinion revolutions. It was assumed that the gears were geometrically ideal with no profile errors or tooth spacing errors. The effect of dynamic loads induced by tooth flexibility and gear inertia was neglected. Uniform line contact between mating gear teeth was also assumed. Material constants and exponents which are used in the analysis were obtained from experimental results. The life and dynamic capacity equations, when simplified by setting the helix angle to zero, reduce to the results which were previously developed for spur gears.

Lewis Research Center,
National Aeronautics and Space Administration
and
U.S. Army Air Mobility R&D Laboratory,
Cleveland, Ohio, June 10, 1975,
505-04.

APPENDIX A

SYMBOLS

a	half of major axis of Hertzian contact, m (in.)
B_1	material constant defined by eq. (B5)
b	half of minor axis of Hertzian contact, m (in.)
c	orthogonal shear stress exponent
E	Young's modulus, N/m^2 (psi)
E_o	defined by eq. (B13)
e	Weibull's exponent
f	face width of tooth (fig. 1), m (in.)
h	depth to critical stress exponent
K', K_1, K_2	constants of proportionality
L	pitting fatigue life, millions of revolutions
L_1	life of a single pinion tooth, millions of revolutions
L_{GP}	gear life in terms of pinion rotations, millions of revolutions
ℓ	involute profile arc length, m (in.)
ℓ_c	length of contact line, m (in.)
N	number of teeth
P	diametral pitch, teeth/meter of pitch diameter (teeth/in.)
p	load-life exponent defined by eq. (B12)
p_b	base pitch, m/tooth (in./tooth)
Q	normal tooth load, N (lb)
q	maximum contact stress, N/m^2 (psi)
r	pitch circle radius, m (in.)
r_a	addendum circle radius, m (in.)
r_b	base circle radius, m (in.)
S	probability of survival; surface area, m^2 ($in.^2$)
V	volume, m^3 ($in.^3$)

W_t	transmitted tangential load, N (lb)
W_{tM}	dynamic capacity of gear-pinion mesh, N (lb)
w	defined by eq. (18)
z_o	depth of occurrence of maximum orthogonal reversing shear stress, m (in.)
XYZ, $\bar{i}\ \bar{j}\ \bar{k}$ xyz, $\bar{n}_1\ \bar{n}_2\ \bar{n}_3$	right-handed orthogonal coordinate systems and associated unit vectors
β_{H1}	heavy-load-zone roll angle, rad
β_{L1}	light-load-zone roll angle, rad
γ	tooth-contact roll angle, rad
δ	precontact roll angle, rad
ζ	length of zone of contact in plane of action, m (in.)
η	millions of stress cycles
θ	base circle roll angle, rad
λ	lead of helix, m (in.)
ρ	principal radius of curvature, m (in.)
$\sum \rho$	curvature sum, m^{-1} ($in.^{-1}$)
σ	Poisson's ratio
τ_o	maximum subsurface orthogonal reversing shear stress, N/m^2 (psi)
φ_t	transverse pressure angle, rad
ψ_b	base helix angle, rad
ω	base helix parameter

Subscripts:

G	gear
H	heavy load
L	light load
M	mesh of pinion and gear
P	pinion
1	driving member
2	driven member

APPENDIX B

FORMULATION OF BASIC HELICAL GEAR LIFE EQUATION

In this appendix, the Lundberg-Palmgren life model is used to obtain a fundamental form which is a starting point for the derivation of the helical gear life formula. Most of the work presented here is in explanation of the method used to obtain the material constant in equation (1). Lundberg and Palmgren did not introduce such a constant of proportionality until their equation had been specialized for use in rolling bearing life prediction.

The basic formulation by Lundberg and Palmgren (ref. 15) was

$$\log \frac{1}{S} \propto \frac{\tau_o^c \eta^e}{z_o^h} V \tag{B1}$$

If a constant of proportionality is used, the result is

$$\log \frac{1}{S} = K' \frac{\tau_o^c \eta^e}{z_o^h} V \tag{B2}$$

Since a relation for fatigue life is wanted, the equation is rearranged. And since there is only one stress cycle per revolution of the gear, the following equation may be written:

$$\eta = L_1 = \left(\frac{\log \frac{1}{S}}{K'} \frac{z_o^h}{\tau_o^c V} \right)^{1/e} \tag{B3}$$

If it is assumed that all lives will be calculated for a 90 percent survival rate,

$$L_1 = \left(\frac{K_1 z_o^h}{\tau_o^c V} \right)^{1/e} \tag{B4}$$

The constant K_1 in this equation must now be determined. The constant K_1 may

be related to the material constant B_1, which was given in reference 20. The following equations were taken from reference 20, which pertains to steel spur gears with uniformly distributed stress along the line of contact between the teeth:

$$L_1 = B_1^p \left(\frac{\ell_1}{\pi}\right)^{-1/e} \sum \rho^{-(c+h-1)/2e_f (c-h-1)/2e_Q - p} \tag{B5}$$

$$V = a z_o \ell_1 \tag{B6}$$

$$z_o = 0.5\, b \tag{B7}$$

$$\tau_o = 0.25\, q \tag{B8}$$

$$q = \frac{2Q}{\pi f b} \tag{B9}$$

$$a = \frac{3}{4} f \tag{B10}$$

$$b = \sqrt{\frac{8Q}{\pi f E_o \sum \rho}} \tag{B11}$$

$$p = \frac{c - h + 1}{2e} \tag{B12}$$

$$E_o = \frac{E}{1 - \sigma^2} = 2.3 \times 10^{11}\ \mathrm{N/m^2} (3.3 \times 10^7\ \mathrm{psi}) \tag{B13}$$

$$c = 10\tfrac{1}{3} \tag{B14}$$

$$h = 2\tfrac{1}{3} \tag{B15}$$

Substitution of equations (B6) to (B12) into equation (B4) and comparing the result with equation (B5) show that the following relation exists between B_1 and K_1:

$$K_1 = \left(\frac{3\pi}{4}\right)(2)^{h-1}(2\pi)^{-c}\left(\frac{\pi E_o}{8}\right)^{(c+h-1)/2} B_1^{(c-h+1)/2} \tag{B16}$$

In reference 20 it was found that $B_1 = 4.08\times10^8$ when newton and meter units are used in equation (B5) and that $B_1 = 102\ 000$ when pound and inch units are used. Since K_1 does not depend on the Weibull exponent, there is no theoretical relation between the constant K_1 and the failure distribution of a sample of test gears. Thus, a constant obtained from bearing tests may also be used in the gear life formula. Finally, using equations (B13) to (B15) yields K_1 equal to 1.43×10^{95} for newton and meter units (3.58×10^{56} for pound and inch units).

APPENDIX C

DERIVATION OF STRESSED VOLUME FOR HELICAL TOOTH

In this appendix the equations describing a helical gear tooth surface are presented. The expression for the differential element of tooth surface area is derived. Then by comparing the expressions for helical gear tooth surface area and spur gear tooth surface area, it is seen how the stressed volume should be written for the helical gear. The parametric equations describing the base helix, which is shown in figure 6, are

$$X = r_b \sin \omega \tag{C1}$$

$$Y = r_b \cos \omega \tag{C2}$$

$$Z = \frac{\lambda}{2\pi} \omega \tag{C3}$$

where X, Y, and Z denote the position coordinates of the base helix traced on the base cylinder in terms of the parameter ω. The position vector of a point on the base helix may be written

$$\overline{P} = X\overline{i} + Y\overline{j} + Z\overline{k} \tag{C4}$$

Let the reference frame xyz have its origin at P, and let a point on an involute profile be located by the position vector $\overline{q}$

$$\overline{q} = x\overline{n}_1 + y\overline{n}_2 \tag{C5}$$

where

$$x = r_b(\sin \theta - \theta \cos \theta) \tag{C6}$$

$$y = r_b(\cos \theta + \theta \sin \theta - 1) \tag{C7}$$

Then the position vector of a point on the surface of the helical tooth is given by

$$\overline{R} = \overline{P} + \overline{q} \tag{C8}$$

Since the position vectors have their basis vectors in different reference frames, a transformation matrix may be used to transform the components of $\bar{q}$ from the xyz frame to the XYZ frame. Therefore, the components of position vector $\bar{R}$ in the XYZ frame may be written as

$$\begin{Bmatrix} R_X \\ R_Y \\ R_Z \end{Bmatrix} = \begin{Bmatrix} X \\ Y \\ Z \end{Bmatrix} + \begin{bmatrix} \cos\omega & \sin\omega & 0 \\ -\sin\omega & \cos\omega & 0 \\ 0 & 0 & 1 \end{bmatrix} \begin{Bmatrix} x \\ y \\ 0 \end{Bmatrix} \tag{C9}$$

The components of $\bar{R}$ in the XYZ frame are found to be

$$R_X = r_b[\sin(\theta + \omega) - \theta \cos(\theta + \omega)] \tag{C10}$$

$$R_Y = r_b[\cos(\theta + \omega) + \theta \cos(\theta + \omega)] \tag{C11}$$

$$R_Z = \frac{\lambda\omega}{2\pi} \tag{C12}$$

These equations describe the helix surface by two parameters, θ and ω. The physical meaning of the two parameters can be seen in figure 7. The equation of the line described if θ is held fixed and ω varied is one of the ω-coordinate lines. Hence, the two parameters of the surface describe the grid mesh on the face of the helical tooth. The grid lines are not mutually perpendicular.

Finally, the surface area element is given by the vector product

$$d\bar{S} = \frac{\partial\bar{R}}{\partial\omega} d\omega \times \frac{\partial\bar{R}}{\partial\theta} d\theta \tag{C13}$$

The result of this vector operation is

$$d\bar{S} = -\frac{\lambda r_b \theta}{2\pi} \cos(\theta + \omega)\bar{i} + \frac{\lambda r_b \theta}{2\pi} \sin(\theta + \omega)\bar{j} + r_b^2 \theta \bar{k}\, d\omega\, d\theta \tag{C14}$$

The magnitude of the surface differential area element is determined by the scalar product as

$$dS = \sqrt{d\bar{S} \cdot d\bar{S}} \tag{C15}$$

The result is

$$dS = r_b\theta \sqrt{\left(\frac{\lambda}{2\pi}\right)^2 + r_b^2}\, d\omega\, d\theta \tag{C16}$$

By using equation (C3), equation (C16) may be written

$$dS = r_b\theta \sqrt{1 + \left(\frac{2\pi r_b}{\lambda}\right)^2}\, dZ\, d\theta \tag{C17}$$

From the geometry of figure 2, the following relation is obtained:

$$\tan \psi_b = \frac{2\pi r_b}{\lambda} \tag{C18}$$

Using equation (C18) in (C17) gives the result

$$dS = r_b\theta \sec \psi_b\, dZ\, d\theta \tag{C19}$$

The expression for surface area of the helical tooth is obtained by integrating equation (C19):

$$S = \sec \psi_b \int_{\theta_1}^{\theta_2} r_b\theta\, d\theta \int_0^f dZ \tag{C20}$$

The term under the first integral is the length ℓ of the involute in the transverse plane. The length ℓ is the arc length along the constant-ω lines of figure 7. The second integral denotes the face width f of the helical gear tooth.

For a spur gear, the volume representation which accounts for the size effect of the material in relation to the extent of the stress field is given in reference 20 by the following equation:

$$V = \frac{3}{4} f z_o \ell_1 \tag{C21}$$

The term ℓ_1 is the length of the involute in the critically loaded zone, while f is the face width. Therefore the product $f\ell_1$ is a representation of the spur gear surface area in the critically loaded zone.

The surface area for spur and helical gears differs only by a factor, sec ψ_b. Therefore, the expression for the stressed volume of the helical gear tooth is written

$$V = \frac{3}{4} f z_o \ell \sec \psi_b \qquad \text{(C22)}$$

APPENDIX D

HELICAL GEAR GEOMETRY NECESSARY FOR CALCULATION OF INVOLUTE PROFILE ARC LENGTH

In reference 20 the equations were given for calculation of the length of involute for which only two teeth are in contact. Equations (D1) to (D10) summarize these equations.

$$\ell_1 = \frac{r_{b1}}{2}\left(\theta_{U1}^2 - \theta_{L1}^2\right) \tag{D1}$$

$$r_{b1} = r_1 \cos \varphi_t \tag{D2}$$

$$\theta_{L1} = \delta_1 + \beta_{L1} \tag{D3}$$

$$\theta_{U1} = \theta_{L1} + \beta_{H1} \tag{D4}$$

$$\delta_1 = \frac{(r_1 + r_2)\sin \varphi_t - \sqrt{r_{a2}^2 - r_{b2}^2}}{r_{b1}} \tag{D5}$$

$$r_{b2} = r_2 \cos \varphi_t \tag{D6}$$

$$\beta_{L1} = \frac{\zeta - p_b}{r_{b1}} \tag{D7}$$

$$\beta_{H1} = \frac{2p_b - \zeta}{r_{b1}} \tag{D8}$$

$$p_b = \frac{2\pi r_{b1}}{N_1} \tag{D9}$$

$$\zeta = \sqrt{r_{a1}^2 - r_{b1}^2} + \sqrt{r_{a2}^2 - r_{b2}^2} - (r_1 + r_2)\sin \varphi_t \tag{D10}$$

If the entire length of the involute is wanted, the following equations should be used for θ_{L1} and θ_{U1} instead of equations (D3) and (D4):

$$\theta_{L1} = \delta_1 \tag{D11}$$

$$\theta_{U1} = \delta_1 + \gamma_1 \tag{D12}$$

where γ_1 is the total increment of pinion roll angle for which there is tooth contact.

$$\gamma_1 = \frac{\zeta}{r_{b1}} \tag{D13}$$

REFERENCES

1. Coleman, W.: Gear Design Considerations. Interdisciplinary Approach to the Lubrication of Concentrated Contacts, P. M. Ku, ed., NASA SP-237, 1970, pp. 551-589.

2. Blok, H.: Surface Temperature Under Extreme-Pressure Lubricating Conditions (Les Temperatures des Surface Dans des Conditions de Graissage Sous Extreme Pression). Proceedings of Second World Petroleum Congress, Paris, Vol. 3, 1937, pp. 471-486.

3. Blok, Harmen: The Postulate About the Constancy of Scoring Temperature. Interdisciplinary Approach to the Lubrication of Concentrated Contacts, P. M. Ku, ed., NASA SP-237, 1970, pp. 153-248.

4. Ishikawa, Jiro; Hayashi, Kunikazu; and Yokoyama, Masaaki: Surface Temperature and Scoring Resistance of Heavy-Duty Gears. J. Eng. Ind., ASME Trans., vol. 96, no. 2, May 1974, pp. 385-390.

5. Rating the Strength of Helical and Herringbone Gear Teeth. AGMA Paper 221.02, Aug. 1966.

6. Shigley, Joseph E.: Mechanical Engineering Design. 2nd ed., McGraw-Hill, 1972, pp. 533-536.

7. Chabert, G.; Dang Tran, T.; and Mathis, R.: An Evaluation of Stresses and Deflections of Spur Gear Teeth Under Strain. J. Eng. Ind., ASME Trans., vol. 96, no. 1, Feb. 1974, pp. 85-93.

8. Wellauer, E. J.; and Seireg, A.: Bending Strength of Gear Teeth by Cantilever Plate Theory. J. Eng. Ind., ASME Trans., vol. 82, ser. B, Aug. 1960, pp. 213-220.

9. Wellauer, E. J.: An Analysis of Factors Used for Strength Rating of Helical Gears: J. Eng. Ind., ASME Trans., vol. 82, ser. B, Aug. 1960, pp. 205-212.

10. Surface Durability (Pitting) of Helical and Herringbone Gear Teeth. AGMA Paper 211.02, July 1965.

11. Information Sheet for Surface Durability (Pitting) of Spur, Helical, Herringbone and Bevel Gear Teeth. AGMA Paper 215.01, Sept. 1966.

12. Ishibashi, Akira; Ueno, Taku; and Tanaka, Shigetada: Surface Durability of Spur Gears at Hertzian Stresses Over Shakedown Limit. J. Eng. Ind., ASME Trans., vol. 96, no. 2, May 1974, pp. 359-372.

13. Schilke, W. E.: The Reliability Evaluation of Transmission Gears. SAE Paper 670725, Sept. 1967.

14. Huffaker, G. E.: Compressive Failures in Transmission Gearing. SAE Trans., vol. 68, 1960, pp. 53-59.

15. Lundberg, G.; and Palmgren, A.: Dynamic Capacity of Rolling Bearings. Ing. Vetanskaps Akad. -Handl., No. 196, 1947.

16. Lundberg, G.; and Palmgren, A.: Dynamic Capacity of Roller Bearings. Ing. Vetanskaps Akad. -Handl., No. 210, 1952.

17. Hayashi, Kunikazu; Anno, Yoshiro; and Aiuchi, Susumu: Allowable Stresses in Gear Teeth Based on the Probability of Failure. ASME Paper 72-PTG-45, Oct. 1972.

18. Bodensieck, E. J.: A Stress-Life-Reliability Rating System for Gear and Rolling-Element Bearing Compressive Stress and Gear Root Bending Stress. AGMA Paper 229.19, Nov. 1974.

19. Rumbarger, John H.; and Leonard, Larry: Derivation of a Fatigue Life Model for Gears. FIRL-F-C2864, Franklin Institute (AD-744504, USAAMRDL-TR-72-14), 1972.

20. Coy, John J.; Townsend, Dennis P.; and Zaretsky, Erwin V.: Analysis of Dynamic Capacity of Low-Contact-Ratio Spur Gears Using Lundberg-Palmgren Theory. NASA TN D-8029, 1975.

21. Townsend, D. P.; and Zaretsky, E. V.: A Life Study of AISI M-50 and Super-Nitralloy Spur Gears with and without Tip Relief. J. Lubri. Tech., ASME Trans., vol. 96, no. 4, Oct. 1974, pp. 583-590.

22. Wellauer, E. J.: Helical and Herringbone Gear Tooth Durability - Derivation of Capacity and Rating Formulas. AGMA Paper 229.06, June 1962.

23. Schmitter, W. P.: The American Gear Manufacturers Association's Surface Durability Rating Standards for Spur, Helical, and Herringbone Gearing - a Recapitulation of their Derivation. AGMA Paper 219.05, June 1955.

24. Matsunaga, T.: Influence of Profile Modification and Lubricant Viscosity on Scoring of Helical Gear. J. Eng. Ind., ASME Trans., vol. 96, no. 1, Feb. 1974, pp. 71-77.

25. Littman, W. E.: The Mechanism of Contact Fatigue. Interdisciplinary Approach to the Lubrication of Concentrated Contacts, P. M. Ku, ed., NASA SP-237, 1970, pp. 309-377.

26. Smith, J. O.; and Liu, Chang K.: Stresses Due to Tangential and Normal Loads on a Elastic Solid with Application to Some Contact Stress Problems. J. Appl. Mech., ASME Trans., vol. 20, no. 2, June 1953, pp. 157-166.

27. Diaconescu, E. N.; Kerrison, G. D.; and MacPherson, P. B.: A New Machine for Studying the Effects of Sliding and Traction and the Fatigue Life of Point Contacts, with Initial Test Results. ASLE Preprint 74LC-5A-3, Oct. 1974.

28. Dudley, Darle W., ed.: Gear Handbook. First ed., McGraw-Hill, 1962, pp. 5-43.

29. Bamberger, E. N.; Harris, T. A.; Kacmarsky, W. M.; Moyer, C. A.; Parker, R. J.; Sherlock, J. J.; and Zaretsky, E. V.: Life Adjustment Factors for Ball and Roller Bearings. An Engineering Design Guide. American Society of Mechanical Engineers, 1971.

TABLE I. - SAMPLE CALCULATION

Symbol	Definition	Equation	Formula	Result
W_t	Transmitted tangential load, N (lb)	-----	Given	1.40×10^5 (31 500)
φ_t	Transverse pressure angle, deg	-----		20
ψ_b	Base helix angle, deg	-----		15
P	Diametral pitch, teeth/cm (teeth/in.)	-----		0.3937 (1)
N_1	Number of pinion teeth	-----		16
N_2	Number of gear teeth	-----		36
---	Speed of pinion, rpm	-----		1000
f	Face width, cm (in.)	-----		7.62 (3.00)
r_1	Pinion pitch radius, cm (in.)	-----		20.32 (8.00)
r_2	Gear pitch radius, cm (in.)	-----		45.72 (18.00)
r_{a1}	Pinion addendum radius, cm (in.)	-----		22.86 (9.00)
r_{a2}	Gear addendum radius, cm (in.)	-----		48.26 (19.00)
r_{b1}	Pinion base circle radius, cm (in.)	(D2)	$r_1 \cos \varphi_t$	19.09 (7.5175)
r_{b2}	Gear base circle radius, cm (in.)	(D6)	$r_2 \cos \varphi_t$	42.96 (16.9145)
$\sum\rho$	Curvature sum, cm^{-1} ($in.^{-1}$)	(8)	$(r_1 + r_2)\cos \psi_b/(r_1 r_2 \sin \varphi_t)$	0.2008 (0.5099)
p_b	Base pitch, cm (in.)	(D9)	$2\pi r b_1/N_1$	7.498 (2.9521)
ζ	Length of zone of action, cm (in.)	(D10)	$\sqrt{r_{a1}^2 - r_{b1}^2} + \sqrt{r_{a2}^2 - r_{b2}^2} - (r_1 + r_2)\sin \varphi_t$	11.96 (4.7104)
----	Transverse contact ratio	-----	ζ/p_b	1.5956
β_{H1}	Roll angle through heavy load zone, rad	(D8)	$(2p_b - \zeta)/r_{b1}$	0.1588
β_{L1}	Roll angle through light load zone, rad	(D7)	$(\zeta - p_b)/r_{b1}$	0.2339
δ_1	Precontact roll angle, rad	(D5)	$\left[(r_1 + r_2)\sin \varphi_t - \sqrt{r_{a2}^2 - r_{b2}^2}\right]\Big/r_{b1}$	0 0317

		Case I	Case II	Case I	Case II	Case I	Case II
ℓ_c	Minimum face width in contact, cm (in.)	(21)	(4)	$f/\cos\psi_b$	$0.95\,\zeta f/p_b\cos\psi_b$	7.889 (3.1058)	11.958 (4.7079)
θ_{L1}	Roll angle at which stress begins, rad	(D3)	(D11)	$\delta_1 + \beta_{L1}$	δ_1	0.2656	0.0317
θ_{U1}	Roll angle at which stress ends, rad	(D4)	(D12)	$\theta_{L1} + \beta_{H1}$	$\delta_1 + \zeta/r_{b1}$	0.4244	0.6583
ℓ	Length of stressed portion of involute, cm (in.)	(D1)		$r_{b1}\left(\theta_{U1}^2 - \theta_{L1}^2\right)/2$		1.046 (0.4119)	4.128 (1.6251)
W_{tP}	Dynamic capacity of single pinion tooth, N (lb)	(10)		$K_2\ell_c\cos\varphi_t\left[f\ell(\cos\psi_b)^{-5.5}\left(\sum\rho\right)^{35/6}\right]^{-2/9}$		3.75×10^6 (844 000)	4.19×10^6 (943 000)
W_{tM}	Dynamic capacity of mesh, N (lb)	(19)		$\left\{N_1\left[1+\left(\frac{N_1}{N_2}\right)^3\right]\right\}^{-2/9} W_{tP}$		1.99×10^6 (447 000)	2.22×10^6 (500 000)
L	System life, millions of pinion revolutions (hr)	(20)		$\left(\frac{W_{tM}}{W_t}\right)^{1.5}$		53.47 (890)	63.15 (1050)

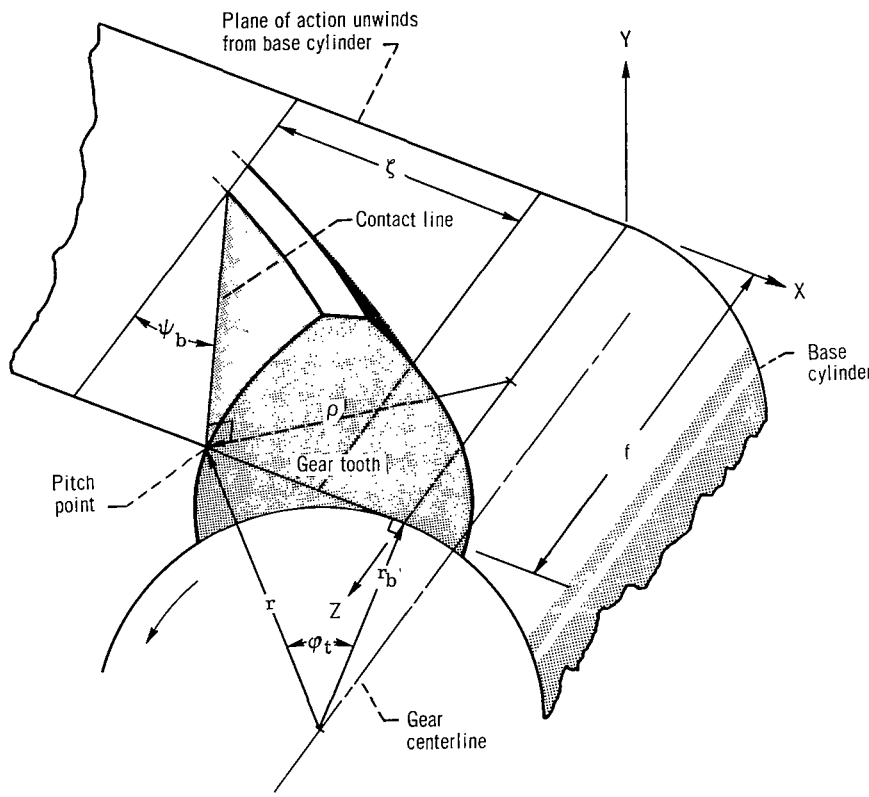

Figure 1. - Exaggerated view of helical gear tooth showing base cylinder and plane of action. Contact line is intersection of tooth face with plane of action. Contact between mating gear teeth occurs on the contact line.

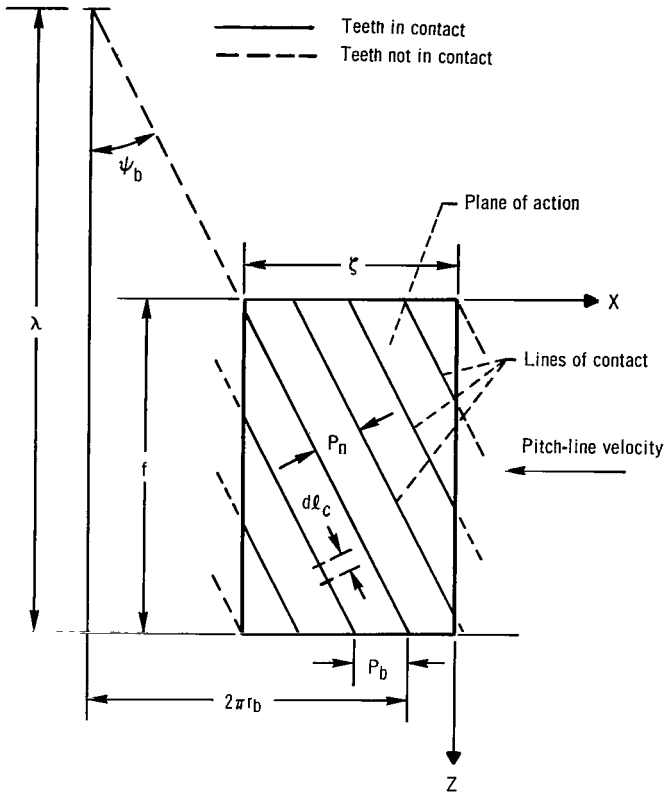

Figure 2. - Zone of contact in plane of action at instant of initial tooth contact.

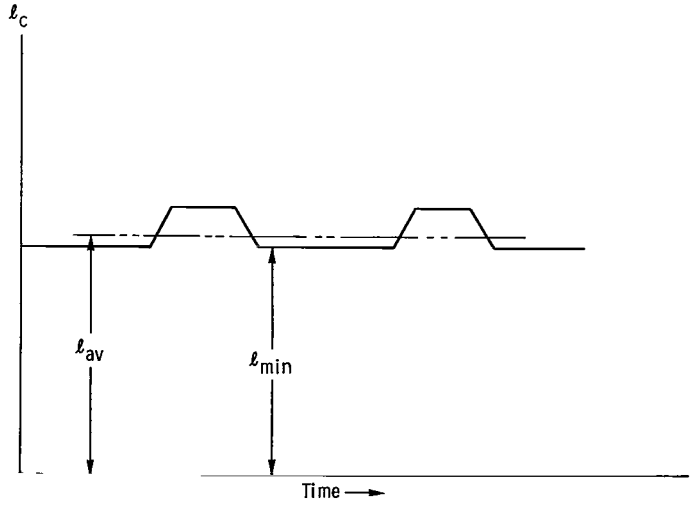

Figure 3. - Typical periodic variation in total length of contact lines in helical gear mesh.

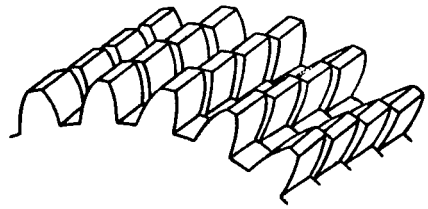

Figure 4. - Stepped spur gears. A helical gear results when there is a large number of very thin gear sections.

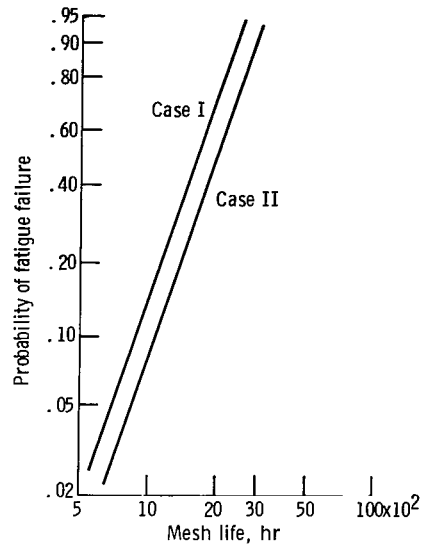

Figure 5. - Theoretical distribution of failures for 16-tooth helical pinion driving 36-tooth gear. Speed, 1000 rpm; helix angle, 15^0; pressure angle, 20^0; maximum Hertzian stress, 119 000 N/cm^2 (173 000 psi); material, 60 Rockwell C hardness steel.

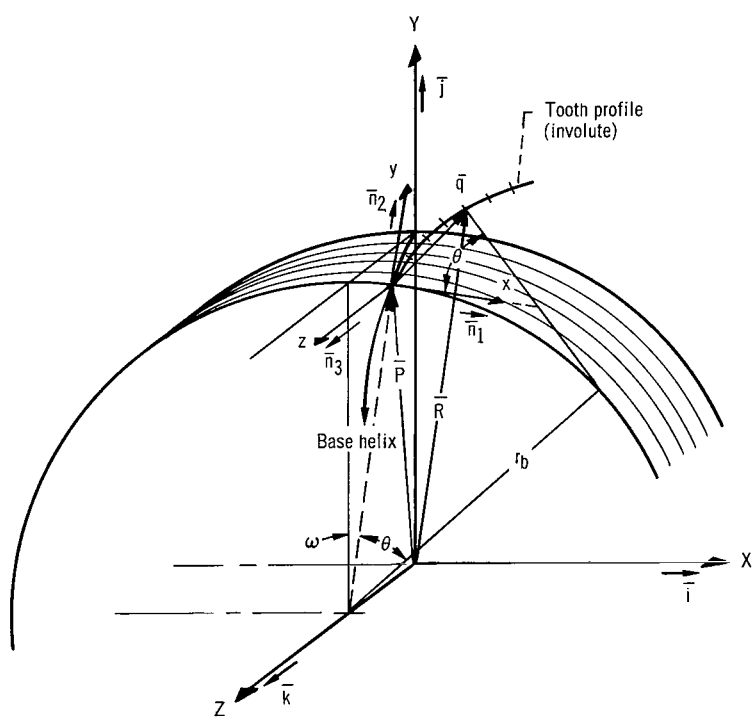

Figure 6. - Helical tooth geometry showing the base helix and a single profile line element.

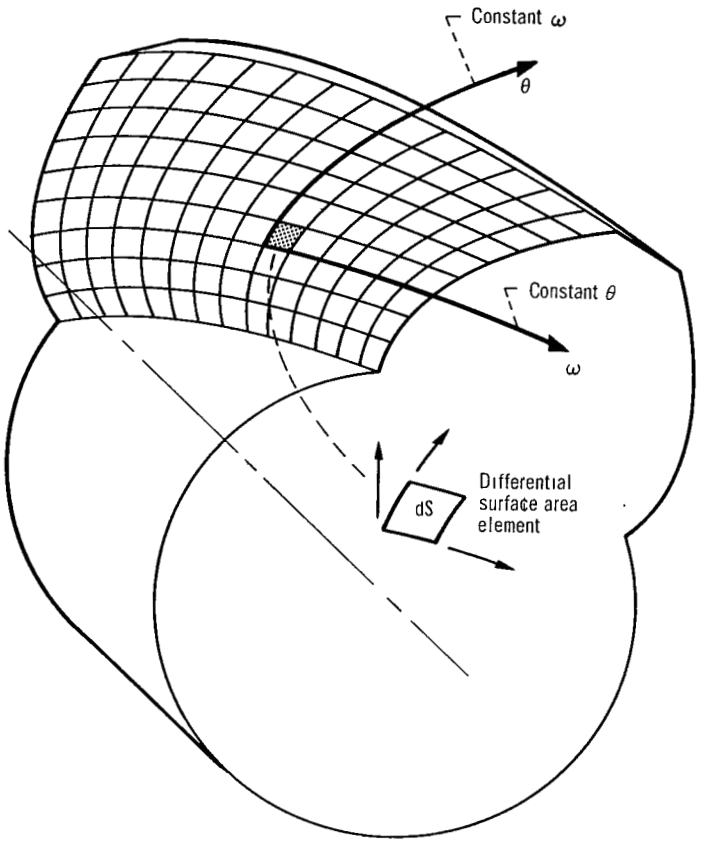

Figure 7. - Lines of constant ω and constant θ scribed on surface of helical gear tooth.

"The aeronautical and space activities of the United States shall be conducted so as to contribute . . . to the expansion of human knowledge of phenomena in the atmosphere and space. The Administration shall provide for the widest practicable and appropriate dissemination of information concerning its activities and the results thereof."

—NATIONAL AERONAUTICS AND SPACE ACT OF 1958

NASA SCIENTIFIC AND TECHNICAL PUBLICATIONS

TECHNICAL REPORTS: Scientific and technical information considered important, complete, and a lasting contribution to existing knowledge.

TECHNICAL NOTES: Information less broad in scope but nevertheless of importance as a contribution to existing knowledge.

TECHNICAL MEMORANDUMS: Information receiving limited distribution because of preliminary data, security classification, or other reasons. Also includes conference proceedings with either limited or unlimited distribution.

CONTRACTOR REPORTS: Scientific and technical information generated under a NASA contract or grant and considered an important contribution to existing knowledge.

TECHNICAL TRANSLATIONS: Information published in a foreign language considered to merit NASA distribution in English.

SPECIAL PUBLICATIONS: Information derived from or of value to NASA activities. Publications include final reports of major projects, monographs, data compilations, handbooks, sourcebooks, and special bibliographies.

TECHNOLOGY UTILIZATION PUBLICATIONS: Information on technology used by NASA that may be of particular interest in commercial and other non-aerospace applications. Publications include Tech Briefs, Technology Utilization Reports and Technology Surveys.

Details on the availability of these publications may be obtained from:

SCIENTIFIC AND TECHNICAL INFORMATION OFFICE

NATIONAL AERONAUTICS AND SPACE ADMINISTRATION

Washington, D.C. 20546